J|A|C|S

A R T I C L E S

Theoretical Analysis of the Electronic Structure and Bonding Stability of the TCNE Dimer Dianion (TCNE)$_2^{2-}$

Jacek Jakowski and Jack Simons*

Contribution from the Chemistry Department and Henry Eyring Center for Theoretical Chemistry, University of Utah, Salt Lake City, Utah 84112

Received April 16, 2003; E-mail: simons@chemistry.utah.edu

Abstract: The (TCNE)$_2^{2-}$ dimer dianion formed by connecting two TCNE$^-$ anions via a four-center, two-electron π-orbital bond is studied using ab initio theoretical methods and a model designed to simulate the stabilization due to surrounding counterions. (TCNE)$_2^{2-}$ is examined as an isolated species and in a solvation environment representative of tetrahydrofuran (THF) solvent. The intrinsic strength of this novel bond and the influences of internal Coulomb repulsions, of solvent stabilization and screening, and of counterion stabilization are all considered. The geometry, electronic and thermodynamic stabilities, electronic absorption spectra, and electron detachment energies of this novel dianion are examined to help understand recent experimental findings. Our findings lead us to conclude that the (TCNE)$_2^{2-}$ dianion's observation in solid materials is likely a result of its stabilization by surrounding countercations. Moreover, our results suggest the dianion is geometrically metastable in THF solution, with a barrier to dissociation into two TCNE$^-$ anions that can be quickly surmounted at room temperature but not at 77 K. This finding is consistent with what is observed in laboratory studies of low- and room-temperature solutions of salts containing this dianion. Finally, we assign two peaks observed (at 77 K in methyl-THF glass) in the UV−vis region to (1) electronic transitions involving the four-center orbitals and (2) detachment of an electron from the four-center π-bonding orbital to generate (TCNE)$_2^-$ + e$^-$.

I. Introduction

Very recently, salts containing the tetracyanoethylene anion TCNE$^-$ have been characterized[1] by X-ray crystallography and visible−ultraviolet (UV−vis) spectroscopy, among other means. The novelty of the salts under discussion is that the X-ray and electron spin resonance (ESR) data strongly suggest they contain anionic centers in which *pairs* of TCNE$^-$ ions are held together as π-bonded dimer dianions having unusually long (ca. 2.9 Å) C−C distances and no unpaired electrons. X-ray data show the dianion units to be oriented as in Figure 1a. Moreover, the theoretical analysis accompanying the experimental effort in ref 1 suggests that the pairs of TCNE$^-$ anions, each containing one electron in its π^* orbital, are bonded via a four-center, two-electron bond[2] as depicted in Figure 1b.

That is, each TCNE$^-$ unit (labeled left (L) and right (R) in Figure 2) has a bonding π and an antibonding π^* orbital. These four orbitals combine, when the two TCNE$^-$ anions are brought into contact as shown in Figure 1, to form two orbitals ($\pi_R + \pi_L$ and $\pi^*_R + \pi^*_L$) that are bonding with respect to the inter-ion coordinate and two orbitals ($\pi_R - \pi_L$ and $\pi^*_R - \pi^*_L$) that are inter-ion antibonding. The ground state of the six-π-electron
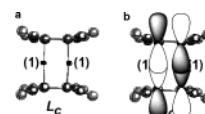

Figure 1. (a) Structure of (TCNE)$_2^{2-}$ (labeled L$_C$ as in ref 1); (b) overlap of singly occupied π^* orbitals on each TCNE$^-$ anion to form four-center, two-electron bond.
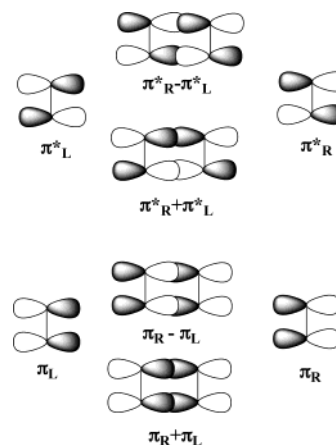

Figure 2. Four π-based four-center molecular orbitals (center) and their origins from the two left (L) and right (R) TCNE$^-$ anions' orbitals.

(TCNE)$_2^{2-}$ dianion has a $(\pi_R + \pi_L)^2 (\pi_R - \pi_L)^2 (\pi^*_R + \pi^*_L)^2$ configuration that produces a bond order of unity for the four-center inter-ion bond. It is the nature of this inter-ion bonding that forms the focus of the present work.

(1) (a) Novoa, J. J.; Lafuente, P.; Del Sesto, R. E.; Miller, J. S. *Angew. Chem., Int. Ed.* **2001**, *40*, 2540−2545. (b) Del Sesto, R. E.; Miller, J. S.; Lafuente, P.; Novoa, J. J. *Chem. Eur. J.* **2002**, *8*, 4894−4908.

(2) Of course, each TCNE$^-$ anion also has a pair of electrons in its bonding π orbital, so the electronic configuration of the six total π electrons is $\pi^2 \pi^2 \pi^{*2}$, with the latter pair forming the bond between the two TCNE$^-$ anions. The four π electrons are not what is forming the inter-TCNE bond; rather, it is the two π^* electrons.
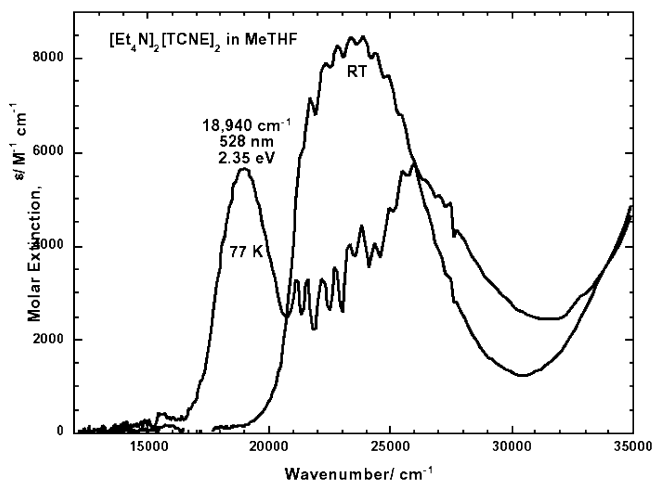
Figure 3. Electronic spectrum of $(TCNE)_2{}^{2-}$ in methyl-tetrahydrofuran at 77 K (as a glassy material) and at room temperature (RT). The absorptions shown at RT are characteristic of the $TCNE^-$ anion (taken from ref 1b).

As noted above, magnetism and ESR studies of such salts show no signature of unpaired electrons, thus supporting the claim that the electrons of the $TCNE^-$ anions are indeed spin-paired as suggested in the above bonding paradigm.[3] Furthermore, the electronic spectra of such salts display two absorption peaks that do not occur in salts containing the $TCNE^-$ anion alone and thus seem to relate specifically to the dianions. These two peaks occur at energies slightly below 20 000 cm^{-1} and above 25 000 cm^{-1}, respectively (their precise peak energies varied depending on the specific countercations). In ref 1 these UV−vis absorptions were assigned to transitions involving the π and π^* orbitals of the $(TCNE)_2{}^{2-}$ dianions,[2] but which orbital transitions are involved in each of the two transitions was not specified.

Finally, when the salts studied in ref 1 are dissolved in methyl-tetrahydrofuran (MeTHF) and subjected to UV−vis spectral analysis, spectra such as shown in Figure 3 are obtained.[4]

An important feature to note about the above spectra is that, at room temperature, the MeTHF UV−vis spectra display no characteristic absorption features in the <20 000 or > 25 000 cm^{-1} ranges. Instead, they show a strong absorption profile ranging between 20 000 and 25 000 cm^{-1} that is characteristic of the $TCNE^-$ anion. However, at liquid nitrogen temperature (where a glassy sample is obtained), the MeTHF solution spectra display the two absorptions that are characteristic of the $(TCNE)_2{}^{2-}$ dianion (<20 000 and > 25 000 cm^{-1}).

This body of experimental data[1,4] and its accompanying theoretical analysis thus support the following notions:

(a) In the solids and in MeTHF solution, $(TCNE)_2{}^{2-}$ is a singlet species (at least at the temperatures studied) bound by a two-electron bond involving π^* orbitals on the two $TCNE^-$

units (as well as by the stabilizing electrostatic potentials generated by the surrounding countercations in the solid and by the solvation and counterion stabilization in MeTHF).

(b) In MeTHF solution, $(TCNE)_2{}^{2-}$ is in equilibrium with 2 $(TCNE)^-$ with the equilibrium strongly favoring $(TCNE)_2{}^{2-}$ at 77 K but favoring 2 $(TCNE)^-$ at room temperature.

In the present contribution, we describe our efforts to further understand (i) the nature and intrinsic strength of the four-center two-electron bond that is thought to bind the two $TCNE^-$ units together; (ii) the role of internal Coulomb repulsion in destabilizing the bonding between the two $TCNE^-$ anions; (iii) the roles of solvent screening and stabilization and of counterion interactions in altering the bonding between the two $TCNE^-$ ions; (iv) the origins of the <20 000 and >25 000 cm^{-1} UV−vis absorptions; and (v) why $(TCNE)_2{}^{2-}$ is stable (or long-lived) in solution at 77 K but dissociates into 2 $TCNE^-$ at room temperature.

In section II, we detail the methods we use (i) to carry out the ab initio calculations, (ii) to model the effects of solvation and of the surrounding ions, and (iii) to estimate the electronic transition energies of $(TCNE)_2{}^{2-}$ in solution. In section IV we summarize our findings, and in section III we discuss the details of our results. The approach we take to analyzing the nature of the bonding in $(TCNE)_2{}^{2-}$ involves (i) first, studying the $(TCNE)_2{}^{2-} \rightarrow 2$ $(TCNE)^-$ energy profile in the absence of any stabilizing solvent or any counterions to determine whether the $(TCNE)_2{}^{2-}$ dianion is stable or metastable and thus might be studied via electrospray mass spectroscopy; (ii) removing the internal Coulomb repulsions between the two anion centers in $(TCNE)_2{}^{2-}$ to gain an estimate of the intrinsic bond strength produced by the two-electron four-center bond; (iii) incorporating screening and stabilization effects of THF solvent to determine the magnitude of these influences, and, finally, (iv) using a simple electrostatic model to estimate the differential stabilizing influence of the surrounding ion environment on $(TCNE)_2{}^{2-}$ compared to 2 $(TCNE)^-$ since such interactions tend to stabilize the dianion more than the two monoanions and thus affect the equilibrium between the two species.

II. Methods

A. Basis Sets Used in the ab Initio Calculations. To make ab initio calculations computationally feasible at a reasonable level of electron correlation, we decided to use atomic orbital basis sets that we denote augsp-cc-pVDZ. These bases retain only the diffuse s and p functions of the full aug-cc-pVDZ bases; they do not retain the full bases' diffuse d-type orbitals. To justify the use of this basis, we verified that our ab initio data (e.g., vertical electron detachment energies, geometries, vibrational frequencies) for the TCNE monomer and its anion obtained with our basis set produce results that are very close to those obtained by others in the aug-cc-pVDZ[5] basis. As a result of this choice of basis, calculations on the TCNE dimer involve 360 Gaussian basis functions.

Because the chosen basis is rather modest, it was important for us to examine the effects of basis set superposition errors (BSSE). Corrections for BSSE (at the UHF, MP2, and MP3 levels of theory) to the interaction energy surfaces of nonsolvated $(TCNE)_2{}^{2-}$ dimer dianions and $(TCNE)_2{}^-$ dimer monoanions were determined for several

(3) It is not possible to exclude the possibility that the electronic configuration of the $(TCNE)_2{}^{2-}$ dianions is not $(\pi_R+\pi_L)^2(\pi_R-\pi_L)^2(\pi^*_R+\pi^*_L)^2$ but a singlet-coupled (because the ESR signature clearly shows no unpaired electrons) $(\pi_R+\pi_L)^2(\pi_R-\pi_L)^2(\pi^*_R+\pi^*_L)^1(\pi^*_R-\pi^*_L)^1$ configuration. However, the fact that the findings presented later in this paper, based upon the former electronic configuration, are consistent with the observed experimental data (including the UV−vis spectra) suggest the closed-shell rather than the singlet open-shell configuration is more likely.

(4) Very recently, another group has examined the same dimer dianion's UV−vis spectra as well as the thermodynamics involved in the ion-pairing process: Lü, J.; Roscokha, S. V.; Kochi, J. K. *J. Am. Chem. Soc.* **2003**, *125*, 12161−12171.

(5) For example, as discussed later, the bases we employ produce dianion-to-anion energy gaps (i.e., vertical electron detachment energies) in good agreement with those found in the following reference where the larger basis mentioned earlier was used: Zakrzewski, V. G.; Dolgounitcheva, O.; Ortiz, J. V. *J. Chem. Phys.* **1996**, *105*, 5872.

distances (R) between the two TCNE units by computing the interaction energy as follows:[6,7]

$$E_{int}(AB) = E(AB) - E_{DBS}(A) - E_{DBS}(B)$$

Here, $E(AB)$ and E_{DBS}(A or B) stand, respectively, for the total energy of the AB dimer and the total energy of the A or B monomer, both computed with the dimer basis set.

B. Unrestricted and Spin-Projected Calculations. On the basis of the findings of ref 1 and considering the bonding picture embodied in Figure 2 where two electrons are assumed to occupy the same four-center π-bonding orbital, we note that the dimer dianion (TCNE)$_2^{2-}$ involves two singlet spin-coupled electrons occupying the ($\pi^*_R + \pi^*_L$) orbital at R values where the two TCNE$^-$ π^* orbitals overlap strongly. However, we need to use a wave function that will allow this electronic configuration to evolve into a singlet-coupled open-shell pair of identical TCNE$^-$ anions at large R.

As is well known, for example in the case of H$_2 \rightarrow$ 2H, it is improper to attempt to describe such homolytic bond cleavage using a single-determinant restricted Hartree−Fock (RHF) reference wave function; such a function simply cannot properly dissociate, although it is capable of treating the bond at shorter R values.

To obtain potential surfaces that can describe the homolytic dissociation of the bond in (TCNE)$_2^{2-}$, we therefore employed unrestricted Hartree−Fock (UHF) and corresponding unrestricted Møller−Plesset (UMP) perturbation theory (up to third order) as implemented in the Gaussian 98[8] program. Because spin contamination was found to be substantial (e.g., for TCNE$^-$, $S(S + 1) = 0.89$ rather than 0.75), we also employed spin projection to purify our (nominally) singlet state for (TCNE)$_2^{2-}$ and our (nominally) doublet state for TCNE$^-$. The spin projections and subsequent MPn energies reported later in this paper were computed using the UHF reference wave function at the UHF-optimized geometries.

C. Energy Surface Scans. In carrying out our potential energy surface determinations, all geometrical degrees of freedom were optimized (i.e., varied to minimize the energy) except for the inter-TCNE$^-$ distance R, which was scanned over distances ranging from 2.5 to 10 Å. The distance R was varied in steps of 0.1 Å in the region between 2.5 and 4.6 Å, and in larger steps at larger R values. Both D_{2h} (with the two TCNE moieties oriented as in Figure 1) and D_{2d} (with the one TCNE rotated by 90°) geometries of (TCNE)$_2^{2-}$ were considered in our calculations, but, as suggested in ref 1, the D_{2d} geometries were found to be energetically less favorable, so they were not pursued further.

Although the optimal geometry of (TCNE)$_2^{2-}$ is rigorously of D_{2h} symmetry, to achieve proper dissociation (at the UHF level and beyond), we used only the two planes of symmetry appropriate to C_{2v} symmetry in our calculations. This was necessary to achieve proper homolytic cleavage of the two-electron four-center π bond discussed in this paper. As a result, our molecular orbitals are not perfectly symmetry-adapted with respect to the plane that reflects one TCNE$^-$ into the other; they are proper eigenfunctions of the plane containing the four carbon atoms involved in the four-center bond and the plane bisecting each TCNE$^-$ anion's central C−C bond.

D. Solvation Effects. Solvent screening and stabilization effects were incorporated by means of the polarized continuum model (PCM) of Tomasi and Persico[9] with tetrahydrofuran as the solvent. We chose THF as our solvent[10] because it is very similar to the MeTHF solvent

used in the experiments of ref 1, but the Gaussian program does not contain explicit PCM parameters for MeTHF.

E. Ion Atmosphere Stabilization Effects. In both the solid state (i.e., the ionic salts studied in ref 1) and MeTHF solution, each (TCNE)$_2^{2-}$ or (TCNE)$^-$ ion is surrounded by other positive and negative ions. In the salts, these ions are arranged in a regular lattice so their stabilizing influence on each (TCNE)$_2^{2-}$ or (TCNE)$^-$ ion can be estimated as was done in ref 1. In MeTHF solution, each anion is also surrounded by an environment of other positive and negative charges, but these ions are not ordered in a regular lattice. Nevertheless, the stabilization energy induced at a site occupied by a (TCNE)$_2^{2-}$ or a (TCNE)$^-$ ion can be estimated using, for example, a Debye−Hückel type theory.[11] As shown later, the incorporation of such effects is important for understanding the differential stabilization of (TCNE)$_2^{2-}$ over (TCNE)$^-$ and for interpreting the temperature dependence of the behavior of (TCNE)$_2^{2-}$ in MeTHF.

F. Electronic Excited States. Electronically excited states of the (TCNE)$_2^{2-}$ dianion in THF solvent were studied at the projected UHF, configuration interaction singles (CIS), configuration interaction singles and doubles (CIS-D),[12] and UMP2 levels of theory. This range of methods was employed to gain a feel for how these energies vary when electron correlation effects are (CIS-D and UMP2) and are not (UHF and CIS) included. It turns out this aspect of the study is important because the electron pair involved in forming the four-center π^* bond has a substantial correlation energy, so only the UMP2 and CIS-D data were found to be capable of explaining the experimental observations. That is, the noncorrelated CIS and UHF predictions of the excitation energies are not in the range of what is seen experimentally, whereas the energy spacings found using UMP2 or CIS-D methods agree rather well with experimental observations.

G. Inter-TCNE$^-$ Vibrational Mode in Solution. Because of the highly nonharmonic form of the dimer dianion's potential along the coordinate R (as shown later in this paper), the inter-fragment vibrational stretching frequencies of (TCNE)$_2^{2-}$ in THF were computed using a sixth-order polynomial fit of the potential curve in the region of its minimum. We used a variational method with Gaussian-type expansion functions for both the BSSE-corrected and uncorrected inter-fragment potentials and obtained 31 and 27 cm^{-1} as the zero-point vibrational corrections, respectively, for the inter-fragment vibrational mode. We note these findings because it is unlikely that the harmonic frequencies for this mode obtained from the ab initio Gaussian code will be of use to experimental chemists for such an anharmonic degree of freedom.

III. Results

A. (TCNE)$_2^{2-}$ in the Absence of Solvation. We first examine the potential energy surface of an isolated (TCNE)$_2^{-2}$ dianion in order to determine whether this species might be susceptible to, for example, electrospray mass spectroscopic detection. The key issues are whether this dianion's energy surface has a minimum and whether the dianion is stable with respect to the corresponding monoanion plus a free electron (i.e., to auto-detachment).

In Figure 4a we show the energies (calculated at the MP3 level with BSSE corrections[13]) of the (TCNE)$_2^-$ anion and the (TCNE)$_2^{2-}$ dianion as functions of the distance R between the centers of the two TCNE units with all other geometrical degrees

(6) van Duijneveldt, F. B.; van Duijneveldt-van de Rijdt, J. G. C. M.; van Lenthe, J. H. *Chem. Rev.* **1994**, *94*, 1873−1885.

(7) Jeziorski, B.; Szalewicz, K. Intermolecular Interactions by Perturbation Theory. In *The Encyclopedia of Computational Chemistry*; von Rague Schleyer, P., Allinger, N. L., Clark, T., Gastaiger, J., Kollman, P. A., Schaefer, H. F., Schreiner, P. A., Eds.; Wiley: Chichester, 1998.

(8) Frisch, M. J.; Trucks, G. W.; Schlegel, H., B.; et al. *Gaussian 98*, Revision A7; Gaussian, Inc.: Pittsburgh, PA, 1998.

(9) Tomasi, J.; Persico, M. *Chem. Rev.* 2027−2094.

(10) We could not use methyl-tetrahydorfuran because the Gaussian 98 program we employ does not contain explicit solvation parameters for this solvent, whereas it does for THF.

(11) See, for example, p 327 of *An Introduction to Statistical Thermodynamics*; Hill, T. L., Ed.; Addison-Wesley: Reading, MA, 1960.

(12) For these calculations, we used the more recent Gaussian 03 suite of codes (Frisch, M. J.; Trucks, G. W.; Schlegel, H. B.; et al. *Gaussian 03*; Gaussian, Inc.: Pittsburgh, PA, 2003.).

(13) We observed negligible changes in the geometry of the anion when BSSE corrections were performed, and we found the BSSE energy corrections for the dimer monoanion to be very near to those of the dimer dianion.
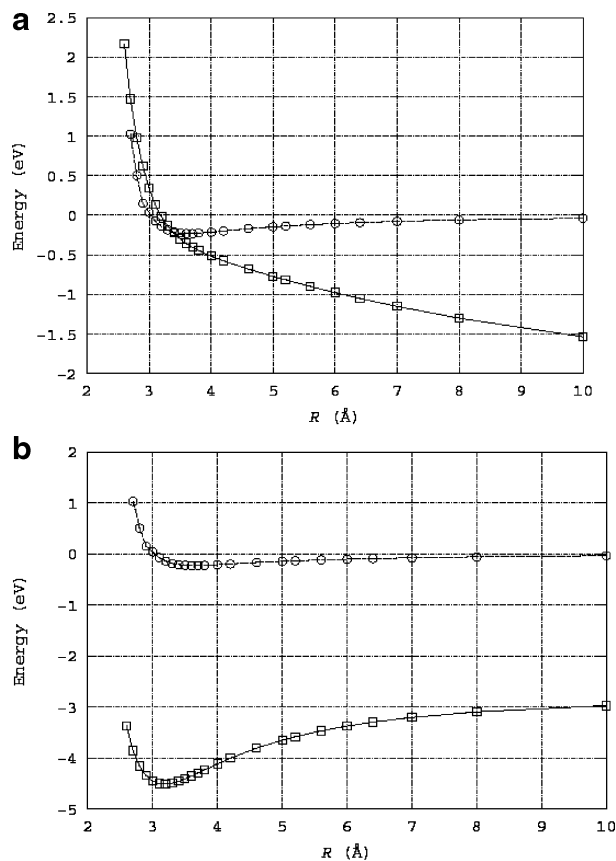
Figure 4. (a) MP3 monoanion and dianion energies (BSSE corrected) as a function of inter-TCNE distance R; (b) same data but with Coulomb repulsion removed from the dianion data.

of freedom adjusted to minimize the energy. In this and subsequent figures, unless otherwise noted, we choose the zero of energy to correspond to the dimer monoanion at $R = \infty$. The dimer dianion potential curve at $R = \infty$ thus lies below zero by an amount corresponding to the electron binding energy of a TCNE$^-$ anion.

The (TCNE)$_2^-$ monoanion shows a potential well characteristic of the one-electron four-center half bond that binds the two TCNE units together. The depth of this well is ca. 0.23 eV or 5 kcal mol^{-1} and has its minimum near 3.6 Å. It should be noted that the salts studied in ref 1, which are assumed to contain (TCNE)$_2^{2-}$ units, show R values near 2.9 Å, so the fact that the R value obtained for the monoanion (3.6 Å) is somewhat longer should not be surprising.

In contrast, the MP3/BSSE dimer dianion potential curve (Figure 4a) shows no minimum, has a form that varies as e^2/R at long R, and is unstable with respect to electron loss (to form the monoanion) at R values shorter than ca. 3.5 Å. These data suggest that it is unlikely that gas-phase electrospray mass spectroscopic probes of (TCNE)$_2^{-2}$ will be successful, for it appears that isolated (TCNE)$_2^{-2}$ is not a stable or metastable species.

To explore to what extent the repulsive behavior of the dianion curve is due to the mutual Coulomb repulsion between the two anions and to uncover any underlying attractive bonding interactions between the two TCNE$^-$ anions, we show in Figure 4b the same (TCNE)$_2^{2-}$ data but with the Coulomb repulsion removed.[14] We remove the repulsion by simply subtracting $14.39/R(\text{Å})$ (in eV) from our ab initio dianion curve of Figure

4a.[15] The data in Figure 4b suggest clearly that if the internal Coulomb repulsion between the two TCNE$^-$ anions were not operative, the dimer dianion would display a bond stronger than that of the (TCNE)$_2^-$ monoanion and, at $R = 3.2$ Å, a bond length shorter than that in (TCNE)$_2^-$.

It is also important to note from Figure 4b that the dianion lies ca. 2.9 eV below the monoanion at large R; this energy difference is the electron detachment energy (DE) of a single TCNE$^-$ anion, and this computed value agrees well with the values obtained by other theoretical and experimental workers.[5]

The above data support that idea that there is a one-electron four-center bond in (TCNE)$_2^-$ and an intrinsically stronger two-electron four-center bond in (TCNE)$_2^{2-}$, but the latter is overwhelmed in the isolated (i.e., not solvated nor stabilized by surrounding countercations) dianion by the Coulomb repulsion of the two (TCNE)$^-$ anions. The results shown in Figure 4b for the (TCNE)$_2^{-2}$ dianion thus suggest that this species may exist as an intact (i.e., chemically bound) entity if its internal Coulomb repulsion were counterbalanced by, for example, solvent screening and/or stabilizations due to the dianion's surrounding ionic environment. So, let us now proceed to estimate such effects on the stability of (TCNE)$_2^{2-}$ and of the corresponding monoanion.

B. PCM Treatment of the (TCNE)$_2^{2-}$ → 2 (TCNE)$^-$ Energy Surface in THF. To attempt to simulate the effects of solvation on the (TCNE)$_2^{2-}$ dianions, we employed the polarized continuum model (PCM). However, in these solvated-species calculations, it was necessary for us to limit our study to the MP2 level because MP3 calculations proved to be prohibitive. Moreover, it would have been computationally prohibitive to explicitly incorporate enough solvent molecules to simulate full solution-phase solvation, so a less atomistic model of solvation such as PCM had to be employed. Finally, as noted earlier, we chose THF as our solvent because it is very similar to the MeTHF solvent used in ref 1.

In Figure 5, we show the results of our MP2/PCM simulations of the monoanion and dianion energies as functions of the inter-fragment separation R defined earlier. Again, we define the zero of energy to correspond to the (TCNE)$_2^-$ monoanion at $R = \infty$.

Note that the large R spacing between the monoanion and dianion curves (>3.6 eV) is larger than it is in the data of Figure 4b (ca. 2.9 eV). This is because the THF solvation differentially stabilizes the TCNE$^-$ anion relative to the neutral TCNE, thus causing the TCNE$^-$ electron binding energy to increase in solution. In other words, the solvation energy of the TCNE$^-$ ion in THF is >0.7 eV.

Although it is not apparent from Figure 5, we also note that at large R the (TCNE)$_2^{2-}$ curve (correctly) varies as $e^2/(\epsilon R)$ with $\epsilon = 7.6$ being the dielectric constant of THF. In contrast, the monoanion curve does not possess the Coulomb repulsion form

(14) This kind of analysis has shown, for example, that the potential energy curves of doubly charged cations such as NF^{2+} or O$_2^{2+}$ are very similar to those of the isoelectronic neutral N$_2$ if one removes from the dication potential the Coulomb repulsion (i.e., if one simply subtracts e^2/R). See, for example: Senekowitsch, J.; Oneil, S. V.; Werner, H.-J.; Knowles, P. J. *J. Phys. B* **1991**, *24*, 1529–1538, and references therein.

(15) This calculation is not meant to produce an accurate representation of the dimer dianion curve either within the solids of ref 1 or in THF solution. It is intended to simply suggest that it is reasonable that Coulomb repulsion is the primary reason for the dianion not displaying a minimum in its potential curve.
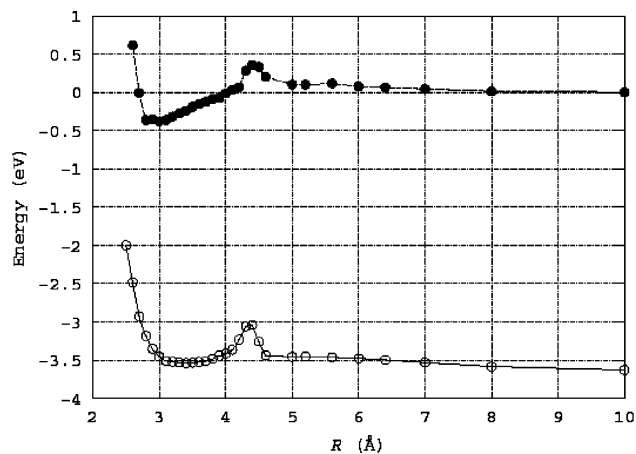
Figure 5. MP2/PCM ab initio energies of monoanion (top) and dianion (bottom) using THF solvent.
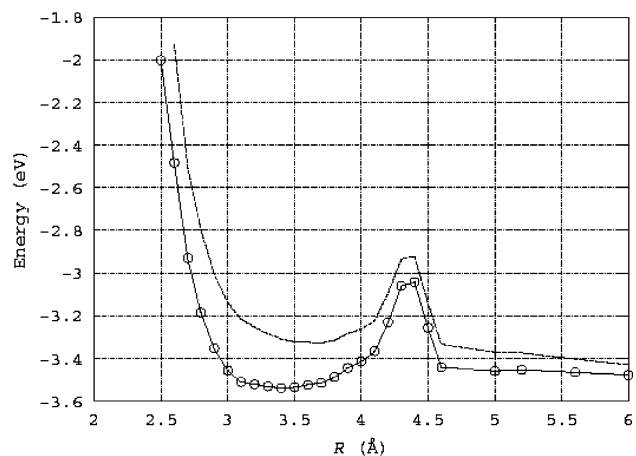

Figure 6. MP2/PCM ab initio energy of the dimer dianion in THF solvent for values of R near the local minimum and solvent-exclusion barrier. The upper curve is obtained when BSSE corrections are included.

at large R. Thus, the dianion curve displays the correct long-range behavior, which allows us to state that the dianion actually lies ca. $3.6 + e^2/(\epsilon 10 \text{ Å}) = 3.8$ eV below 2 (TCNE)$^-$ at infinite R. In other words, 3.8 eV is our best estimate of the electron binding energy for a (TCNE)$^-$ anion in THF solution.

At R values near the minimum in the (TCNE)$_2^{2-}$ curve, the electron detachment energy decreases (from ca. 3.8 eV at infinite R) to ca. 3.25 eV. This energy thus provides our estimate of the photodetachment energy of the intact (TCNE)$_2^{2-}$ dianion in THF.

Note that both the monoanion and dianion curves in Figure 5 have barriers near 4.4 Å, while the dianion has its minimum near $R = 3.4$ Å, and the monoanion has its minimum near $R = 3$ Å. In Figure 6 we show in more detail the part of the dianion energy curve near its minimum to focus on the region where the two-electron four-center bond is most likely operative. Clearly, there is a barrier of ca. 0.5 eV or 11 kcal mol^{-1} on the (TCNE)$_2^{2-}$ surface near $R = 4.4$ Å and a broad minimum near $R = 3.4$ Å. When BSSE corrections are included within this MP2/PCM level calculation, the barrier height decreases to 0.4 eV or 9 kcal mol^{-1} and the minimum shifts to $R = 3.7$ Å. This minimum does not occur at 2.9 Å as seen in the salts of ref 1, but this is not surprising because the data presented in Figures 5 and 6 relate to the dianion in THF solution, not in the solid state.

The fact that a barrier occurs on the (TCNE)$_2^{2-}$ surface is not at all unexpected; the $(e^2/(\epsilon R))$ repulsion at long R combined with the intrinsic attraction due to the four-center bonding at smaller R can certainly cause such a barrier. However, it is unlikely that this competition between Coulomb attraction and chemical bonding is the only source of the barrier because, as Figure 5 shows, the (TCNE)$_2^-$ curve also has a small barrier and no Coulomb repulsion is operative for this monoanion. It is thus likely that solvent interactions also contribute to the barriers found for the monoanion and dianion. That is, we believe the barriers likely arise from two sources: (1) the competition between the Coulomb repulsion between the two TCNE$^-$ anions (operative for the dianion only) and the stabilizing bonding interactions that form at smaller R as the π^* orbitals on the two TCNE$^-$ anions overlap; and (2) changes in how the PCM solvent surrounds the two separated TCNE$^-$ ions at larger R compared to the π^*-bonded (TCNE)$_2^{2-}$ at smaller R.

We attempted to further quantify the role of Coulomb repulsions by carrying out a series of calculations on nonsolvated (TCNE)$_2^{2-}$ in which the atomic charges on the four carbon atoms involved in the four-center two-electron π^* bond were varied from 6.0 to 6.25.[16] We know from past experience[17] that one can incorporate additional partial positive charges into the Hamiltonian to energetically stabilize an electronically unstable state. In the absence of solvation, (TCNE)$_2^{2-}$ is indeed unstable with respect to electron detachment at small R values. However, as the charges on the four carbon atoms are increased beyond 6.0, the (TCNE)$_2^{2-}$ is differentially stabilized with respect to the (TCNE)$_2^-$ monoanion, eventually rendering the dianion stable. Such artificial stabilization forms the basis of the well-known stabilization method[18] that has been widely used to study metastable species. In the present application, we used the stabilization method to try to approximate the stabilization caused by differential solvation of the (TCNE)$_2^{2-}$ dianions. We found that for carbon charges near 6.20 the dianion's potential curve had a barrier near 4.5 Å and a minimum near 3.5 Å, very much as seen in Figures 5 and 6. Moreover, for this range of charges, the (TCNE)$_2^{2-}$ to (TCNE)$_2^-$ electron detachment energy was ca. 4 eV at large R and ca. 3.7 eV at $R = 3.5$ Å, a bit larger than seen in Figure 5. So, these simple model data suggest that part of the origin of the barrier on the (TCNE)$_2^{2-}$ surface indeed lies in the competition between the four-center two-electron bonding and the (reduced by solvation) Coulomb repulsion between the two anionic centers.

Thus far, our simulations suggest that (i) gas-phase (TCNE)$_2^{2-}$ is not geometrically stable and thus is unlikely to be seen in mass spectroscopic experiments; (ii) if stabilization (e.g., by solvation as in THF solution) fully or mostly screens the internal Coulomb repulsion in (TCNE)$_2^{2-}$, this dianion should be geometrically metastable (i.e., will have a barrier on its energy surface) and stable with respect to autodetachment.

However, even when THF solvation is included in our simulations, the (TCNE)$_2^{2-}$ dianion at its local-minimum R

(16) At a carbon charge of 6.25 the total charge of the (TCNE)$_2^{2-}$ has been reduced by one full charge but the number of electrons remains the same as in (TCNE)$_2^{2-}$, so this does not mutate the dianion into the monoanion. Instead, it produces a potential that can more tightly bind the electrons to the nuclear framework.
(17) Simons, J. *J. Chem. Phys.* **1981**, *75*, 2465−2467. Frey, R.; Simons, J. *J. Chem. Phys.* **1986**, *84*, 4462−4469.
(18) Hazi, A. U.; Taylor, H. S. *Phys. Rev. A* **1970**, *1*, 1109.

value is predicted[19] to lie (see Figure 6) ca. 0.4 eV above 2 (TCNE)$^-$. As we discuss in the following section, this energy difference is too large to be consistent with the experimental observations about (TCNE)$_2{}^{2-}$ and 2 (TCNE)$^-$ being in equilibrium and showing the temperature dependence noted in the Introduction.

C. Debye−Hückel Type Treatment of Ionic Environment and Kinetic Stability of (TCNE)$_2{}^{2-}$ at Various Temperatures. It is useful to note that a 9.2 kcal mol^{-1} barrier (see Figure 6) and an inter-fragment vibrational frequency in the 60 cm^{-1} range[20] are consistent with an equilibrium rate of fragmentation (i.e., (TCNE)$_2{}^{2-}$ → 2 TCNE$^-$) of ca. 1.8×10^{12} s^{-1} exp($-9.2 \times 505/T$(K)). At $T = 298$ K and $T = 77$ K, these rates turn out to be 3×10^5 and 10^{-14} s^{-1}, respectively. These estimates suggest that the (TCNE)$_2{}^{2-}$ dianion should be kinetically stable in THF solution at 77 K, but at room temperature should rapidly decompose into two monoanions. This, indeed, is what is seen experimentally[1,4] Using the same barrier and inter-fragment vibrational frequency, we estimate that at $T = 135$ K, the dianion should dissociate at a rate of ca. 0.002 s^{-1}, so it should persist in solution for approximately 10 min. This is a prediction that may be tested in future laboratory studies in which the spectral features are monitored at a range of temperatures.

Although the rates of dissociation of the (TCNE)$_2{}^{2-}$ dianion at 77 and 298 K are in line with the experimental observations, the prediction that (TCNE)$_2{}^{2-}$ lies 0.4 eV above 2 (TCNE)$^-$ is not.[4] In fact, in solution the dissociation (TCNE)$_2{}^{2-}$ → 2 (TCNE)$^-$ is found to be endothermic with $\Delta H = 9-10$ kcal mol^{-1} and with $\Delta S = 36-41$ cal mol^{-1} K^{-1}, not exothermic by 0.4 eV or 9 kcal mol^{-1} as our findings (thus far) suggest.

What is missing from the energy profiles shown in Figures 5 and 6 when applied to the (TCNE)$_2{}^{2-}$ → 2 (TCNE)$^-$ system in THF are the effects of the atmosphere of ions that surround each anion and dianion. To account for the influence of such an ion atmosphere on the relative stabilities of (TCNE)$_2{}^{2-}$ and 2 (TCNE)$^-$, we resort to the Debye−Hückel model. This model[11] estimates the change in free energy δG that accompanies placing an ion of charge Z and radius α into a solution having dielectric constant ϵ and having an ionic strength I as $\delta G/RT = -Z^2 s\kappa/(1 + \kappa\alpha)$. Here, s is the distance at which the inter-ion Coulomb interaction $e^2/\epsilon s$ is equal to kT ($s = 1.67 \times 10^5/\epsilon T$ in Å when T is inserted in degrees K), R is the ideal gas constant (1.98 cal mol^{-1} K^{-1}), and κ is the inverse of the so-called Debye length and is given as $\kappa = 50.29[I/(\epsilon T)]^{1/2}$ in Å^{-1}. The ionic strength is defined as $I = 1/2\sum_J C_J Z_J^2$ where C_J is the molar concentration of the ions of charge Z_J and the sum is taken over all ions in the solution. Clearly, these ion atmosphere effects will differentially stabilize the (TCNE)$_2{}^{2-}$ dianion relative to the two (TCNE)$^-$ monoanions because of the Z^2 dependence in δG.

Unfortunately, the Debye−Hückel model is rigorously applicable under ionic strength and temperature conditions that our system does not obey. Nevertheless, we show below how the concepts of this model can be adapted to our situation, but first let us examine some of the crucial parameters that appear
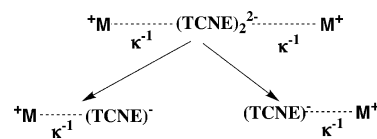
(19) We obtain this estimate by using the $R = 6$ Å energy of -3.4 eV, the R_e energy of -3.3 eV, and the $R = 6$ Å Coulomb repulsion (to extrapolate the energy to $R = \infty$) of 0.32 eV. That is, the energy difference is [0.32 + 3.4] $-$ 3.3 = 0.42 eV.

(20) As noted earlier, this frequency was obtained by solving the one-dimensional (R) Schrödinger equation using the potential shown in Figure 6 for the inter-fragment vibrations of the two (TCNE)$^-$ anions.

Figure 7. Illustration of countercations located κ^{-1} from mono- and dianions.

in the Debye−Hückel equation to understand why such an adaptation is needed.

Using 7.6 as the dielectric constant of THF, the values of the length parameter s at 100, 200, and 300 K are 220, 110, and 73 Å, respectively. The physical meaning of s is it gives the distance at which inter-ion Coulomb interactions ($e^2/(\epsilon s)$) are equal to the thermal energy kT. Two other length parameters are important to consider: the Debye length κ^{-1} and the mean distance r between ions in solution if the ions were randomly distributed. Most of the experimental studies carried out on solutions of the ions in refs 1and 4 involved concentrations in the 10^{-3} molar range, so we use $I = 10^{-3}$ as the ionic strength. This choice produces κ^{-1} values of 17, 25, and 30 Å at 100, 200, and 300 K, respectively. Using this same ionic strength, one can estimate the average inter-ion distance by $r = 11.8$ Å/$(CN)^{1/3}$ where C is the molar concentration of the salt dissolved in THF and N is the number of ions each salt molecule dissociates into (i.e., $N = 3$ if M$_2{}^+$(TCNE)$_2{}^{2-}$ dissociates into 2 M$^+$ + (TCNE)$_2{}^{2-}$ and $N = 4$ if it dissociates into 2 M$^+$ + 2 (TCNE)$^-$). For these possibilities for N, we obtain $r = 75-82$ Å.

Because the distance s over which the Coulomb potentials exceed kT is comparable to or greater than the average (if random) distance r between ions, one should expect appreciable ordering of the ions. That is, the distribution will be nonrandom and will involve a radially nonuniform distribution of ions with those of opposite charge nearest to any given ion. Such a distribution of ions about other ions is exactly what the Debye−Hückel model is supposed to treat, and it produces a radial distribution of counterions peaked at a distance of κ^{-1} around each ion. However, two critical assumptions of this theory are that (i) $\kappa\alpha \ll 1$ (i.e., the ion radius α should be a small fraction of the Debye length κ^{-1}) and (ii) $\kappa^{-1} \gg s$ (i.e., the Debye length should be larger than the distance over which Coulomb interactions are comparable to kT). Considering the X-ray crystallography determined size of a (TCNE)$^-$ anion, it seems unreasonable for α for (TCNE)$^-$ or for (TCNE)$_2{}^{2-}$ to be any larger than ca. 5 Å or smaller than 3 Å. Thus, it is likely that the radius of (TCNE)$_2{}^{2-}$ or of (TCNE)$^-$ is small compared to κ^{-1} (recall κ^{-1} ranges from 17 to 30 Å). However, it is not true that κ^{-1} exceeds s (which ranges from 73 to 220 Å). Therefore, it is not proper to straightforwardly apply the Debye−Hückel formula to determine the difference $\delta\delta G$ in free energy required to place one (TCNE)$_2{}^{2-}$ into the salt solution compared to that needed to place two (TCNE)$^-$ ions into the same solution.

Although the Debye−Hückel formula for δG cannot be used for the reasons detailed above, we now attempt to utilize what this model tells us about the ion clouds that surround (TCNE)$_2{}^{2-}$ or (TCNE)$^-$ ions in the THF solution at 100, 200, or 300 K. It suggests that each (TCNE)$^-$ ion is surrounded, at a distance of ca. κ^{-1}, by one countercation (M$^+$) and that each (TCNE)$_2{}^{2-}$ ion is surrounded by two M$^+$ cations at a distance of ca. κ^{-1}, as shown in Figure 7.

The energy of the dianion relative to that of the two monoanions is already contained in the 0.4 eV value (see Figure 6) mentioned earlier. The Coulomb interaction energy difference appropriate to the $(TCNE)_2^{2-} \rightarrow 2 (TCNE)^-$ case as suggested in Figure 7 is computed[21] as $2 \times 2e^2/\kappa^{-1} - e^2/(2\kappa^{-1}) - 2[e^2/\kappa^{-1}] = 1.5 \ e^2/\kappa^{-1}$. Using $\kappa^{-1} = 17, 25,$ and 30 Å, we thus obtain stabilization energies of 1.27, 0.86, and 0.72 eV, respectively, for $T = 100, 200,$ and 300 K. These stabilization energies relate to the differential ion-atmosphere stabilization of the doubly charged $(TCNE)_2^{2-}$ in excess of that of two $(TCNE)^-$ ions.

Let us now see what the implications of the above analysis are. As stated earlier, our PCM-based modeling of $(TCNE)_2^{2-} \rightarrow 2 (TCNE)^-$ incorrectly predicts this reaction to be exothermic by 0.4 eV or 9 kcal mol⁻¹. Using the observed[4] $\Delta S = 40$ cal mol⁻¹ K⁻¹ and incorporating the above ion-atmosphere stabilization estimates, we can estimate ΔG for the dissociation reaction (in the presence of solvent and of ion atmospheres) as follows: $\Delta G = -9 - T (0.04) + (29, 20,$ or 17 for $T = 100,$ 200, or 300 K) kcal mol⁻¹. This gives $\Delta G = 16$ kcal mol⁻¹ at $T = 100$ K, $+3$ kcal mol⁻¹ at 200 K, and -4 kcal mol⁻¹ at 300 K. These free energies correspond to equilibrium constants ($-RT \ln K = \Delta G$) for the dissociation reaction $(TCNE)_2^{2-} \rightarrow 2 (TCNE)^-$ of $10^{-35}, 5 \times 10^{-4},$ and 8×10^2 at 100, 200, and 300 K, respectively. We should remark that the above Debye–Hückel-based analysis is intended to offer only suggestions rather than quantitatively accurate predictions. Even so, its predictions seem to be in line with what is seen experimentally; the above equilibrium favors $(TCNE)_2^{2-}$ at 77 K and favors 2 $(TCNE)^-$ at room temperature. It also predicts that both the dianion and monoanions should be present in appreciable concentrations at some temperature above 100 and below 200 K. This prediction can, of course, be tested in the lab.

D. Electronic Transitions of $(TCNE)_2^{2-}$ in THF at Low Temperature. First, we note, as shown in Figure 5, that, near the equilibrium geometry of the $(TCNE)_2^{2-}$ dianion (i.e., in the 3.4–3.7 Å range), the THF-solvated dimer monoanion lies ca. 3.0–3.5 eV higher in energy at the MP2 level of theory. It turns out that the BSSE corrections to the monoanion and dianion curves in this region of R values are nearly identical, so this prediction of the detachment energy is also obtained when BSSE corrections are made. However, when this detachment energy is estimated using the uncorrelated CIS method or by subtracting the UHF energies of the dianion and monoanion, significantly different values are obtained (i.e., values that are not at all close to what is seen experimentally). This suggests that the difference in the correlation energy $(TCNE)_2^{2-}$ and $(TCNE)_2^-$ is substantial and thus needs to be adequately treated. For this reason, we found it essential to compute detachment energies and electronic excitation energies using correlated methods (e.g., the CIS-D or MP2 approaches) to achieve any reasonable interpretation of the experimental data shown in Figure 3.

Returning to the correlated CIS-D and MP2 findings, we conclude that the transition that vertically detaches an electron[22] from the dianion (near $R = 3.4$ Å) to form the monoanion should occur at ca. 24 200–28 200 cm⁻¹ in THF. This finding suggests that at least some of the absorption shown in Figure 3 within the peak lying above 25 000 cm⁻¹ might be associated with photodetachment of the dianion. This prediction should be tested in the laboratory by searching for evidence of ejected electrons or the appearance of paramagnetic $(TCNE)_2^-$ ions when the exciting photon source is tuned to this transition.

To determine what the lower-energy transition of Figure 3 arises from, we investigated the low-lying excited electronic states of the $(TCNE)_2^{2-}$ dianion in THF. In particular, we performed UHF, CIS, CIS-D, and MP2 calculations[23] on several such excited states and found two optically allowed states in the energy range shown in Figure 3. For the reasons explained in discussing the vertical electron detachment energies, we found that only the correlated (MP2 and CIS-D) data produced reliable estimates (i.e., excitation energies in the range observed in Figure 3).

In the region near the minimum on the dianion's energy curve shown in Figure 6 in THF, the first excited state was found to lie (vertically) 20 100 cm⁻¹ (CIS-D) or 21 600 cm⁻¹ (MP2) above the ground state and to involve promotion of an electron from the orbital labeled $(\pi^*_L + \pi^*_R)$ in Figure 2 to an excited orbital of $(\pi^*_R - \pi^*_L)$ character. The second excited state was found to lie 30 900 cm⁻¹ (CIS-D) or 27 900 cm⁻¹ (MP2) above the ground state and to involve promotion of an electron from the orbital of $(\pi_R - \pi_L)$ character into one of $(\pi^*_R - \pi^*_L)$ character (see Figure 2). The fact that the second transition is predicted to lie above the vertical detachment energy (24 200–28 200 cm⁻¹) may be a reflection of the level of theory we have been able to apply to these excited states. For example, we note that our lowest excited state (at 20 100 to 21 600 cm⁻¹) lies ca. 2000–3000 cm⁻¹ above the low-energy peak in Figure 3, so our second peak could also be too high by an equal amount. As a result, we are not able to say with confidence that there should be a second bound excited state. However, we do feel confident in suggesting that the lower-energy peak shown in Figure 3 likely corresponds to the lower-energy excited state we find (at 20 100 to 21 600 cm⁻¹), whereas the higher-energy peak in Figure 3 could have contributions from vertical electron detachment (near 24 200–28 200 cm⁻¹) as noted above and from a second bound excited state lying near the detachment threshold.

IV. Summary

Our ab initio investigation of the dimer dianion formed by connecting two TCNE⁻ anions via a four-center, two-electron π-orbital bond suggests the following:

1. The dianion is geometrically unstable (i.e., has no minimum in its energy curve) as an isolated species, so it is unlikely to be detected in electrospray mass spectroscopic studies.

2. The dianion is locally stable in solvents such as THF where the equilibrium inter-anion distance is ca. 3.4–3.7 Å.

3. In THF, there is a barrier to fragmentation of $(TCNE)_2^{2-}$ into 2 TCNE⁻ of ca. 9 kcal mol⁻¹.

(21) We ignore the ca. 3 Å spacing between the two (TCNE)⁻ units compared to κ^{-1}, and we do not include any solvent dielectric screening because it was included in the calculations leading to the 0.4 eV energy difference obtained from Figure 6.

(22) The energies used in this estimate correspond to vertically detaching an electron to form an unsolvated zero-kinetic-energy free electron plus a (TCNE)₂⁻ monoanion.

(23) These calculations were performed by altering the α and β spin–orbital occupations of the ground state dianion, using these altered occupations to initiate a UHF calculation, after which MP2 corrections were computed. We should note that we found correlation contributions to the excitation energies of these states to be large. As noted elsewhere in this text, if these states are examined at the UHF or singly excited configuration interaction (CIS) level, one does not achieve very reasonable values of the excitation energies.

4. Rapid passage over this barrier occurs at room temperature, thus allowing the dimer dianion to dissociate in ca. 10^{-5} s.

5. In THF at 77 K, the rate of passage over this barrier renders the dimer dianion kinetically very long-lived.

6. The ca. 19 000 cm^{-1} peak in the 77 K UV−visible spectra of MeTHF solutions of salts containing $(TCNE)_2^{2-}$ is likely due to excitation of the dimer dianion from its $(\pi^*_R+\pi^*_L)$ to its $(\pi^*_R-\pi^*_L)$ orbital.

7. The >25 000 cm^{-1} peak in the 77 K spectra may be due to photodetachment from $(TCNE)_2^{2-}$ to form $(TCNE)_2^- + e^-$ or to excitation from a $(\pi_R-\pi_L)$ orbital to a $(\pi^*_R-\pi^*_L)$ orbital of $(TCNE)_2^{2-}$ or to a combination of both processes.

8. Inclusion of ion-atmosphere differential stabilization of $(TCNE)_2^{2-}$ over 2 $(TCNE)^-$, combined with PCM treatment of solvent screening and an ab initio treatment of the potential energy surface, produces a Gibbs free energy profile that favors $(TCNE)_2^{2-}$ at 100 K (and below) and favors 2 $(TCNE)^-$ at room temperature.